Consonant diminution of lattice and electronic coupling between a film and a substrate: Pb on Ge(100)

Pei-Wen Chen,[1] Yu-Hsuan Lu,[1] Tay-Rong Chang,[1] Chi-Bin Wang,[1] Li-Yen Liang,[1] Chung-Huang Lin,[1] Cheng-Maw Cheng,[2] Ku-Ding Tsuei,[1,2] H.-T. Jeng,[1,3] and S.-J. Tang[1,2,*]

[1]*Department of Physics, National Tsing Hua University, Hsinchu 30013, Taiwan*
[2]*National Synchrotron Radiation Research Center, Hsinchu 30076, Taiwan*
[3]*Institute of Physics, Academia Sinica, Nankang, Taipei 11529, Taiwan*

The dependence on thickness of electronic and lattice structures of Pb films deposited on Ge(100) substrate was investigated with angle-resolved photoemission spectroscopy and low-energy electron diffraction. Pb films grew in the (111) surface direction with two (1×1) domains rotated $90°$ relative to each other despite a square lattice of Ge(100); correspondingly, the heavy-hole band edge of Ge does not interact with quantum-well–state bands of Pb films. Symmetry arguments in terms of orbitals of Pb quantum-well states and Ge band edges correlate the consonant diminution of lattice and electronic coupling between the film and the substrate.

Atomically uniform metal films are important for industrial applications and scientific investigation. A preliminary condition for the layer-by-layer growth of uniform films is generally a match between lattices of a film and its substrate. This case commonly applies for metal/metal systems,[1] of which the most successful is Ag/Fe(100);[2] there, uniform Ag films can grow epitaxially in direction (100) up to 100 monolayers (MLs) with the precision of an atomic layer. In contrast, metal films were found to grow uniformly on a semiconductor surface despite a large lattice mismatch[3–6] through subtle control of the growth, such as mild annealing after deposition[3,4] or making a reconstructed surface become a wetting layer for the succeeding growth.[5,6] The important role of the electrons in the growth of a thin film was indicated in an "electron-growth model," taking into account the effects of quantum confinement, charge spilling, and interface-induced Friedel oscillations.[7–10] Quantum-well states (QWSs) have been shown theoretically to be responsible for the surface energies of thin films, which further determine the critical or magical thickness.[8,10] Both lattices and electrons are hence critical for the growth of a thin film.

Pb films on Ge(100), a typical system with a large lattice mismatch, have been investigated with scattering of He atoms[11] and x-ray diffraction,[12] revealing that Pb films grew layer by layer with orientation (111) at a low substrate temperature and that the monatomic step height between terraces depends on the number of grown layers as a result of oscillatory relaxation. In addition to the lattice side, it would be interesting and important to probe the electronic structures of Pb films on Ge(100), as electrons confined in the films, as mentioned previously, are likewise essential for the growth of a thin film. Moreover, as a consequence of quantum-size effects, the properties of thin films are directly related to the energy positions of QWSs.[13,14] In this work, we therefore used angle-resolved photoemission spectroscopy to measure systematically the thickness-dependent electronic structures of Pb films on Ge(100) and made low-energy electron diffraction (LEED) measurements to investigate the correlation between the electronic and the lattice structure during epitaxial growth.

In our experiment, Pb overlayers were grown on an *n*-type doped Ge(100) surface terminated with about 1 ML of Pb to form a c(4 × 8) surface. The deposition and subsequent measurements were performed with the substrate maintained at 133 K. The thickness of a Pb film quoted later excludes the ML of the c(4 × 8) phase. Discrete evolution of the quantum-well peaks with increasing Pb coverage, as observed with angle-resolved photoemission in the direction of normal emission [Fig. 1(a)], enables absolute determination of the film thickness. For photoemission measurements, we used photons with an energy of 21.2 eV from a He lamp or synchrotron radiation from beamlines 21B1-U9 and 03A1 at the National Synchrotron Radiation Research Center in Taiwan.

The first-principles calculations are based on the generalized gradient approximation[15] using the full-potential projected augmented wave method[16] as implemented in the Vienna *ab initio* simulation package.[17] The band structures of bulk Ge were calculated using a 12 × 12 × 12 *k*-point mesh over the Brillouin zone (BZ) with a cutoff energy of 173.81 eV. The Pb films are simulated by free-standing Pb(111) slabs (1–10 layers) with a vacuum thickness lager than 10 Å separating the slabs. For the QWSs of the Pb slabs, the dispersions of the energy bands were calculated using a 10 × 10 × 1 *k*-point mesh over the two-dimensional BZ with a cutoff energy of 97.97 eV. The spin-orbit coupling is included self-consistently in all calculations.

Figure 1(a) shows the energy distribution curves (EDCs) of QWSs at normal emission for Pb films of a thickness from 0 to 10 MLs on the Pb/Ge(100)-c(4 × 8) surface. Each EDC was measured after deposition of Pb for 1 min at a steady rate of ∼0.2 ML/min. The QWS peaks have maximum intensity at integer layers, of which the corresponding EDCs are indicated in blue (color online). Indicated with double arrows are the QWS peaks of adjacent quantum numbers corresponding to the same thickness. It is clear from the spectrum that when the intensity of the QWS peak corresponding to *N* MLs decreases, the peak corresponding to *N* + 1 MLs begins to emerge. This behavior demonstrates that these films grow layer by layer. According to our thickness calibration, the first QWS peak to emerge is at 2 MLs. The energy positions of QWS peaks evolve with increasing thickness in an alternating manner from 2 to 10 MLs; the QWSs associated with odd layers are nearer the Fermi level than are those associated with even layers.
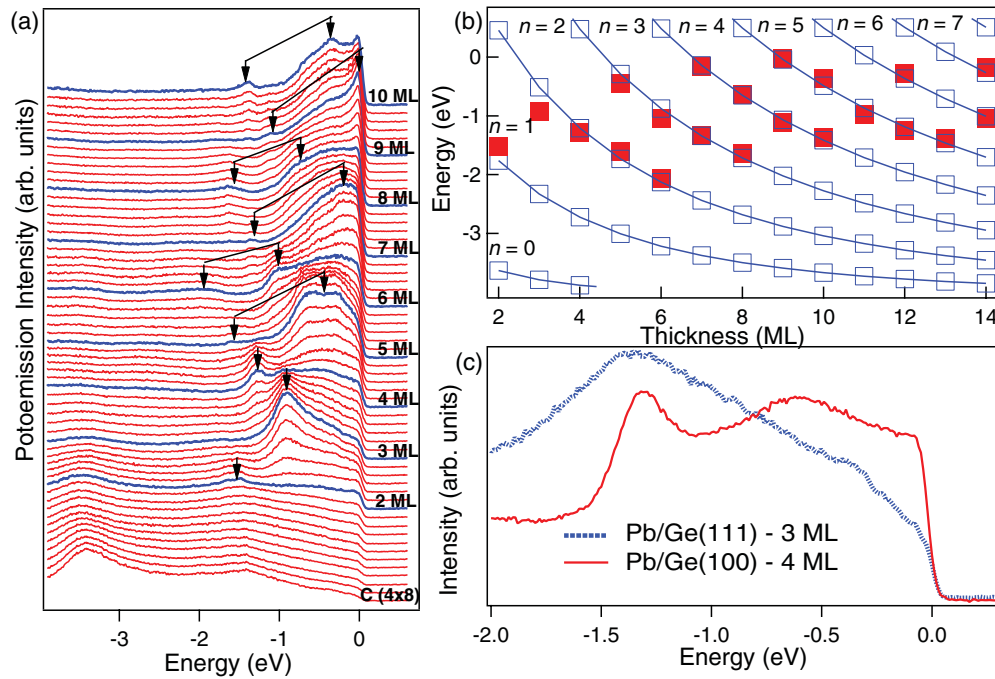
FIG. 1. (Color online) (a) Photoemission spectra at normal emission recorded for Pb films of thickness $N = 0$–10 MLs on Ge(100). (b) Energies of quantum-well peaks at normal emission for quantum numbers $n = 0$–7 over the thickness range $N = 2$–14. The solid (red) squares are experimental results. The open squares and the curves are from a fit. (c) Comparison of the QWS line shape between 3 MLs Pb on Ge(111) and 4 MLs Pb on Ge(100).

The peak positions of QWSs in Fig. 1(a) were further analyzed according to the Bohr-Sommerfeld quantization rule with a linear phase-shift model. Figure 1(b) shows that the data and the model match satisfactorily with varied quantum numbers n. In Fig. 1(a), the QWS peaks within an energy range of -1.5 to about -1 eV exhibit, despite their small intensities, narrower line widths than supposed compared with those of the QWSs for Pb films on Ge(111).

Figure 1(c) shows a comparison of line shape between the QWSs of Pb films on Ge(100) and those of Pb films on Ge(111)[18,19] at the same energy position, which reveals a large contrast in the line width. As the valence maximum of nondoped bulk Ge is roughly at 0.17 eV below Fermi level,[19] those QWSs observed in Fig. 1(a), within the energy range -1.5 to about -1 eV, are expected to be resonances with large line widths like those of the QWSs for Pb/Ge(111) in Fig. 1(c). Although the large lattice mismatch between the substrate surface and the overlayer may induce increase reflectivity at the interface that could then lead to the formation of a sharp resonance, the observed large contrast between these two systems, Pb/Ge(100) and Pb/Ge(111), with the common large lattice mismatch indicates a distinct nature between them.

Figure 2 shows the dependence on thickness of a LEED pattern from a clean two-domain Ge(100)-2 × 1 surface, two-domain Pb/Ge(100)-c(4 × 8) up to 10 MLs. Overall, Pb films grow in surface direction (111) on top of a c(4 × 8) wetting layer with two (1 × 1) domains rotated 90° relative to each other despite a square lattice of Ge(100), which is at 45° with respect to both domains. At 2 MLs, at which the QWS peak was initially observed in photoemission spectra, the

12 LEED spots, indicated with 12 small circles, corresponding to these two (111) domains emerge and become more intense and clearer with increasing thickness. We can consider the lattice structures of the two-domain Pb(111) films to be nearly isotropic. Also shown in Fig. 2 are the surface BZs for Ge surface (100) and a two-domain Pb film (111) superimposed on the corresponding LEED patterns.

Figure 3(a) shows the energy-band dispersions of QWSs along the direction at 15° with respect to both major symmetry directions $\bar{\Gamma}\bar{M}$ and $\bar{\Gamma}\bar{K}$ for Pb films at coverages of 8, 9, and 10 MLs. On the left side of Fig. 3(a), the superimposed solid curves are the calculated Ge bulk band edges, heavy hole (HH), light hole (LH), and split off (SO), in the symmetry direction from $\bar{\Gamma}$ to $\bar{X}$. On the right side of Fig. 3(a), the expected subbands of QWSs for free-standing Pb films based on calculations are superimposed on the data for thicknesses of 8 MLs (broken curves), 9 MLs (solid curves), and 10 MLs (dotted curves). The energy positions of these Pb subbands are determined by those of the QWSs derived from the model fit in Fig. 1(b).

Two striking features are associated with those energy-band dispersions. First, crossing points between the QWS band and the Ge HH band edge, as enclosed with circles, reveal no electron–electron interaction between each other—as opposed to the interactions evident with a Ge LH and a SO band edge, which distort the Pb QWS subbands.[3,19] Second, at coverage of 9 MLs, the QWS band splits at an off-normal position above the LH band edge, as indicated by the rectangular box in Fig. 3(a). Compared with the calculated Pb QWS subbands superimposing onto the experimental photoemission data, the
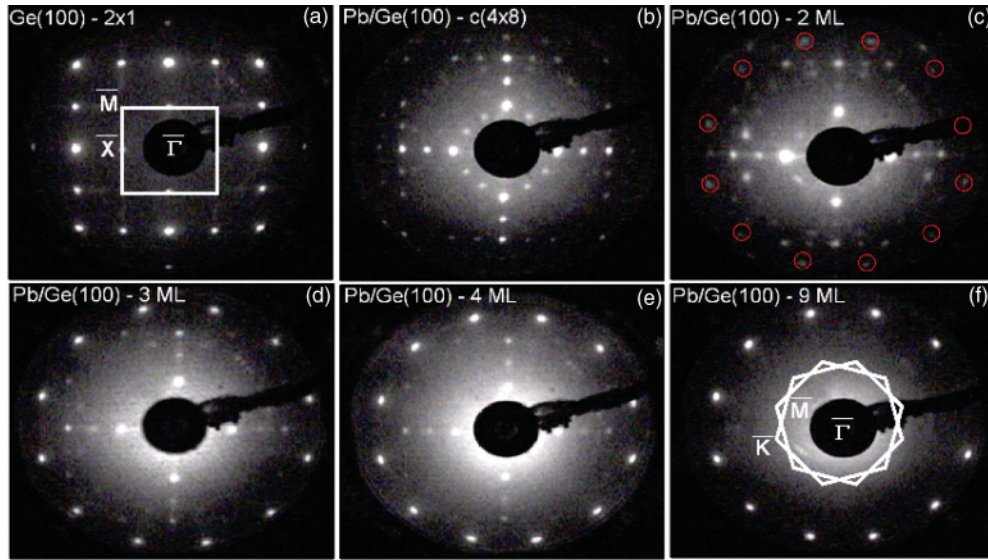
FIG. 2. (Color online) LEED patterns, recorded with a beam energy of 40 eV, from (a) Ge(100)-2 × 1, (b) Pb/Ge(111)-c(4 × 8), and (c) 2 MLs, (d) 3 MLs, (e) 4 MLs, and (f) 9 MLs of Pb overlayers.

two split bands originate from the QWS bands at 8 and 10 MLs. Pb films of 8 and 10 MLs hence coexist with that at coverage of 9 MLs, further implying greater stability of Pb films at even layers than at odd layers.

As shown in Fig. 3(b), the QWS bands of Pb films at coverages 5, 7, and 9 MLs all exhibit the same split structures above the LH band edge. The energy positions of QWSs, as shown in Fig. 1(b), for 5, 7, and 9 MLs are all near the

Fermi level. Therefore, they have relatively larger values of total electron energies than do their adjacent even layers, which in turn deduce to the negative values of the second derivative, indicating unstable layers.[10,13] Similarly split bands were observed for Ag films on Ge(111) or Si(111) surfaces,[3,20] but only at noninteger layers: the two split bands represent a linear combination of the bands from layers N and $N + 1$. Such cases are distinct from Pb films on Ge(100), in which
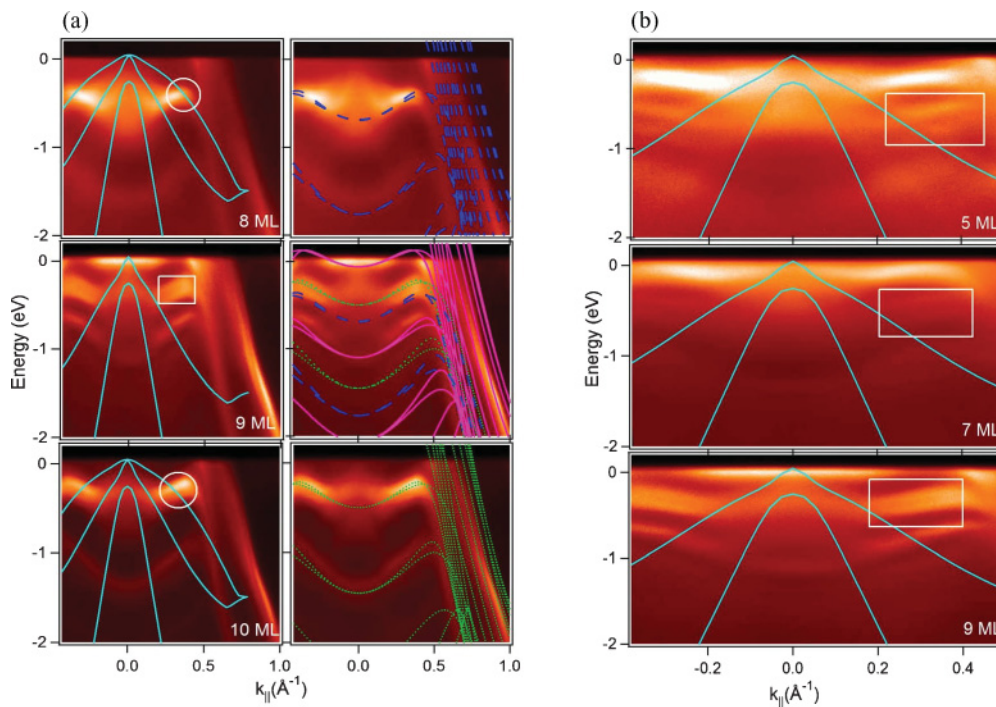

FIG. 3. (Color online) Angle-resolved photoemission data presented as grayscale images as a function of energy and $k_\parallel$ for (a) 8, 9, and 10 MLs and (b) 5, 7, and 9 MLs of Pb on Ge(100).
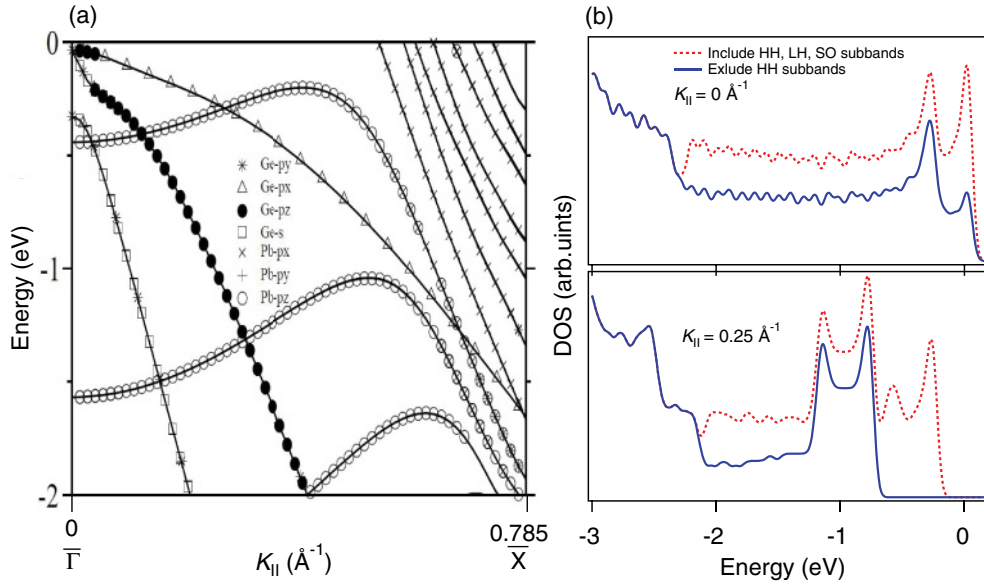
FIG. 4. (Color online) Calculated results for (a) energy-band dispersions of QWSs for Pb (111) films at 10 MLs and Ge band edges in the same directions and for (b) one-dimensional density of states (DOS) for bulk Ge projected on the (100) surface at $k_\parallel = 0$ and 0.25 Å^{-1}.

the split bands, from layers $N + 1$ and $N - 1$, occur at only unstable odd-integer layers N. The lack of interaction between the Pb QWS and the Ge HH band edge is explicable through the matrix element of interaction potentials $\langle \Psi_{\mathrm{Pb}} | V_i | \Psi_{\mathrm{Ge}} \rangle$, with $i = 1, 2$, and 3 for the three Ge valence bands, through a symmetry consideration.[3,18]

Figure 4(a) shows the QWS subbands calculated for 10-ML films, as well as the calculated Ge band edges with their orbital symmetries indicated by symbols. The orbital symmetries of the Pb QWS and the Ge HH band edge in the $k_\parallel$ range near the crossing points have types P_z and P_x, respectively. Due to misalignment $\pm 45°$ between the two domains of Pb(111) films and the square lattice of the Ge(100) surface, the interaction potential is regarded as being isotropic on surface plane xy or independent of the azimuthal angle. The matrix element thus must be zero because of the orthogonal relation. In contrast, the matrix elements for the interaction between the QWS band and two other Ge band edges—LH (P_z type) and SO (mixture of S and P_y type)—are nonzero. According to the calculated result, all Ge HH subbands have type P_x; if they are neglected, a gap in the Ge bulk continuum would form. For that reason, the QWS peaks become sharper above the LH band edge to reveal the layer resolution as shown in Fig. 3(b).

Figures 4(b) and 4(c) show the calculated one-dimensional charge density of states for bulk Ge projected to direction (100), including and excluding those contributed from the HH subbands. A relative gap in the range of roughly -2 eV to about -1 eV is revealed, whether at the surface zone center ($k_\parallel = 0$) or at an off-normal position ($k_\parallel = 0.25$ Å^{-1}). For this reason, our observation, from either the normal emission spectra in Figs. 1(a) and 1(c) or the Pb QWS subband for 10 MLs in Fig. 3(a), arises that the line shape of QWSs becomes narrower within this energy range because of decreased electron–electron scattering between the QWS holes and the Ge bulk continuum.[3]

In summary, we found a consistent decrease in coupling between a Pb film and its Ge(100) substrate in terms of both the lattice and the electrons. For the former, the Pb film grows in direction (111) with two domains rotated $\pm 45°$ with respect to the Ge(100) lattice. For the latter, the Ge HH band edge has no interaction with the Pb QWS bands when they mutually cross. A simple symmetry argument correlates the decreased coupling in both aspects, which further manifests the indispensible relationship between the electrons and the lattice. The results of this work correspond satisfactorily to the preceding argument about the important role of electron–electron hybridization between a film and its substrate for the parallel growth of a one-domain Pb(111) film on Ge(111) despite the large lattice mismatch.[18] In that argument, the alignment of the symmetry axis between the film and the substrate would cause maximum hybridization so as to decrease the energy of the system. For Pb films on Ge(100), the observed rotation $\pm 45°$ of Pb(111) films relative to the symmetry axis of Ge(100) thus implies weaker hybridization, which is confirmed by the lack of interaction between the Pb QWS bands and the Ge HH edge. As is well known, the surface energy of a (111) close-packed surface is the least among the surfaces of a face-centered cubic crystal. For this reason, Pb films grow in direction (111) on a noninteracting substrate.[21,22] In our case, the large lattice mismatch between Pb and Ge causes the growth of film (100) on substrate surface (100) to be unfavorable, whereas hybridization favors it. Nature apparently has a subtle way of attaining minimum energy for the growth of a (111) film simply by making the substrate less interacting.

*sjtang@phys.nthu.edu.tw

[1] T.-C. Chiang, Surf. Sci. Rep. **39**, 181 (2000); M. Milun, P. Pervan, and D. P. Woodruff, Rep. Prog. Phys. **65**, 99 (2002); P. Pervana and M. Milun, Surf. Sci. **603**, 1378 (2009).

[2] J. J. Paggel, T. Miller, and T.-C. Chiang, Science **283**, 1709 (1999).

[3] S.-J. Tang, L. Basile, T. Miller, and T.-C. Chiang, Phys. Rev. Lett. **93**, 216804 (2004).

[4] A. R. Smith, K. J. Chao, Q. Niu, and C. K. Shih, Science **273**, 226 (1996).

[5] M. Upton, C. M. Wei, M. Y. Chou, T. Miller, and T.-C. Chiang, Phys. Rev. Lett. **93**, 026802 (2004).

[6] M. Hupalo, V. Yeh, L. Berbil-Bautista, S. Kremmer, E. Abram, and M. C. Tringides, Phys. Rev. B **64**, 155307 (2001).

[7] Z. Y. Zhang, Q. Niu, and C.-K. Shih, Phys. Rev. Lett. **80**, 5381 (1998).

[8] C. M. Wei and M. Y. Chou, Phys. Rev. B **66**, 233408 (2002).

[9] Y. Jia, B. Wu, C. Li, T. L. Einstein, H. H. Weitering, and Z. Zhang, Phys. Rev. Lett. **105**, 066101 (2010).

[10] Y. Jia, B. Wu, H. H. Weitering, and Z. Zhang, Phys. Rev. B **74**, 035433 (2006).

[11] A. Crottini, D. Cvetko, L. Floreano, R. Gotter, A. Morgante, and F. Tommasini, Phys. Rev. Lett. **79**, 1527 (1997).

[12] L. Floreano, D. Cvetko, F. Bruno, G. Bavdek, A. Cossaro, R. Gotter, A. Verdini, and A. Morgante, Prog. Surf. Sci. **72**, 135 (2003).

[13] D.-A. Luh, T. Miller, J. J. Paggel, M. Y. Chou, and T.-C. Chiang, Science **292**, 1131 (2001).

[14] Y. Guo, Y.-F. Zhang, X.-Y. Bao, T.-Z. Han, Z. Tang, L.-X. Zhang, W.-G. Zhu, E. G. Wang, Q. Niu, Z. Q. Qiu, J.-F. Jia, Z.-X. Zhao, and Q.-K. Xue, Science **306**, 1915 (2004).

[15] J. P. Perdew, K. Burke, and M. Ernzerhof, Phys. Rev. Lett. **77**, 3865 (1996).

[16] G. Kresse and J. Joubert, Phys. Rev. B **59**, 1758 (1999).

[17] G. Kress and J. Hafner, Phys. Rev. B **48**, 13115 (1993).

[18] S.-J. Tang, C.-Y. Lee, C.-C. Huang, T.-R. Chang, C.-M. Cheng, K.-D. Tsuei, H.-T. Jeng, V. Yeh, and T.-C. Chiang, Phys. Rev. Lett. **107**, 066802 (2011).

[19] S.-J. Tang, C.-Y. Lee, C.-C. Huang, T.-R. Chang, C.-M. Cheng, K.-D. Tsuei, and H.-T. Jeng, Appl. Phys. Lett. **96**, 103106 (2010).

[20] N. J. Speer, S.-J. Tang, T. Miller, and T.-C. Chiang, Science **314**, 804 (2006).

[21] Y. Liu, J. J. Paggel, M. H. Upton, T. Miller, and T.-C. Chiang, Phys. Rev. B **78**, 235437 (2008).

[22] J. H. Dil, T. U. Kampen, B. Hülsen, T. Seyller, and K. Horn, Phys. Rev. B **75**, 161401(R) (2007).